

See discussions, stats, and author profiles for this publication at: <https://www.researchgate.net/publication/275153622>

New Method of Quantitative Determination of the Carbon Source in Blast Furnace Flue Dust

ARTICLE *in* ENERGY & FUELS · NOVEMBER 2014

Impact Factor: 2.79 · DOI: 10.1021/ef501863r

CITATION

1

READS

38

6 AUTHORS, INCLUDING:



Jie Yu

Imperial College London

11 PUBLICATIONS 32 CITATIONS

SEE PROFILE



Lushi Sun

Huazhong University of Science and Technology

152 PUBLICATIONS 841 CITATIONS

SEE PROFILE



Song Hu

Washington University in St. Louis

126 PUBLICATIONS 2,447 CITATIONS

SEE PROFILE



Yi Wang

Zhejiang University

310 PUBLICATIONS 3,918 CITATIONS

SEE PROFILE

New Method of Quantitative Determination of the Carbon Source in Blast Furnace Flue Dust

Jie Yu, Lushi Sun,* Jun Xiang, Song Hu, Sheng Su, and Yi Wang

State Key Laboratory of Coal Combustion, Huazhong University of Science and Technology, Wuhan, Hubei 430074, People's Republic of China

ABSTRACT: The unconsumed pulverized coal and coke in flue dusts from two blast furnaces (BFs) were investigated in this paper. The percentage of unconsumed pulverized coal and coke were determined by means of chemical and petrographical microanalyses, which were time-consuming, requiring special expertise, and cannot be practiced routinely. Therefore, a simplified quantification method was proposed. The percentage of these materials in the BF flue dust samples was established on the basis of a suitable calibration using char and coke standards by Raman spectroscopy. The ratios of I_D/I_G , I_V/I_G , and I_{2D}/I_G were used to estimate constituents of the BF flue dust. The amount of unconsumed pulverized coal in 1BF and 2BF was 9.7 and 11.6%, respectively, by means of petrographical microanalysis, and that in 1BF and 2BF established by Raman spectroscopy was in the ranges of 8–10 and 10.5–12%, respectively. The results showed that Raman spectroscopy was a relatively rapid and effective monitoring technique for the purpose of differentiation between coke and unconsumed pulverized coal in BF flue dust.

1. INTRODUCTION

Replacement of metallurgical coke by pulverized coal injected into a blast furnace (BF) is considered as an indispensable and vitally important technology in the ironmaking process, from the view points of reducing costs by decreasing the coke rate and also prolonging the life of the coke oven. Initially, coal injection rates were low, typically from 40 to 90 kg/t of hot metal. An increased understanding of pulverized coal injection technology (PCI) has contributed to higher coke substitution rates, with some BF operating with over 200 kg/t of hot metal reported today,¹ representing about 40% of the total fuels used in common operation of BF. However, operation at a high coal injection rate has been found to cause a number of detrimental changes in BF operation, such as reduced permeability of BF and higher carbon contents in the BF flue dust.² As the injection rate increases, coal combustibility tends to decrease, resulting in unburnt coal fines, char, and ash exiting the “raceway”. Unconsumed coal may eventually be entrained by the gas flow and carried up into the stack, where they can affect burden permeability. Furthermore, unconsumed coal has been found to be associated with the coke fines in flue dust. Akiyama and Kajiwara³ have found that the amount of smaller sized coke fines in the “deadman” increased with increasing coal injection rates, presumably because of the increased momentum of the gas flow in BF caused by rapid volatile evolution.

To obtain a solid basis for keeping stable operation, high production, and low energy consumption in BF, it would be desirable for BF operators to differentiate between the various carbonaceous materials in BF flue dust. Gupta et al.⁴ used a chemical analysis method to study the characteristics of flue dust from three BFs. They found that coke fines were mainly associated with flue dust in size ranges greater than 90 μm and that greater than 250 μm was composed exclusively of coke fines. However, this method did not typically reveal different types of carbonaceous materials in BF flue dust. The most reliable mean to analyze the flue dust at the present time is petrographical microanalysis.^{5,6} The differentiation between carbonaceous

materials is based on overall morphology, particle shape, and degree of development of optical anisotropy revealed by interference contrast. Wu et al.² studied the unconsumed fine coke and pulverized coal in BF flue dust by means of petrographical microanalysis. In that study, the unconsumed fine coal was found in styles of completely unconsumed coal, undeformed coal, deformed coal, and residue coal, while the unconsumed fine coke were divided into a block structure, hemophilic silk carbon, flowing structure, slice structure, granule inlay structure, and residue coke. However, petrographical microanalysis is time-consuming and requires special expertise. Therefore, alternative approaches have been proposed. Machado et al.⁷ used the X-ray diffraction technique in combination with chemical analysis as a standard procedure to identify and differentiate the char and coke structures. Raman spectroscopy has been proven to provide both qualitative and quantitative information on microcrystallite size distribution and ordering of a wide variety of carbon.^{8–10} It was thought that carbonaceous materials existed as the mixture of graphite-like structure and amorphous structure. Various carbonaceous materials have different proportions of graphite-like structure and amorphous structure and, thus, different Raman spectra. The parameters derived from Raman spectra, such as I_D/I_G , I_V/I_G , and I_{2D}/I_G , can be used to determine the degree of graphitization for carbonaceous materials.⁹ The main advantages of Raman are time-saving, efficient, and accurate; moreover, it can reduce manpower cost significantly.

The aim of this study is to establish the proportion of different types of carbonaceous materials (char and coke fines) in BF flue dust by Raman spectroscopy and verify the results by petrographical microanalysis. An attempt has been made to establish the relationship between I_D/I_G , I_V/I_G , and I_{2D}/I_G with the amount of unconsumed coal in BF flue dust.

Received: August 19, 2014

Revised: October 1, 2014

Published: October 1, 2014

2. EXPERIMENTAL SECTION

The methodology conducted in this study was composed of (1) production of char samples in a fixed tube furnace, (2) chemical and granulometry analyses, (3) scanning electron microscopy (SEM) analysis and petrographical microanalysis, (4) Raman analysis of synthetic mixtures, and (5) quantification of the proportion of char and coke fines in BF dust samples.

2.1. Preparation of Samples. Coal samples (1BF-PCI and 2BF-PCI) were obtained from two BFs in the Wuhan Iron and Steel Corporation. Flue dust samples (1BF-dust and 2BF-dust) were collected from the two BFs during the PCI operations. Metallurgical coke samples (1BF-MC and 2BF-MC) were taken from operating BF using the core-drilling technique.¹¹ The drilled BF material was cooled in nitrogen. The slag and iron were separated from the coke. The operating conditions are shown in Table 1, and chemical analyses of coal, coke, and BF flue dust are shown in Table 2.

Table 1. Blast Furnace Operating Conditions

operating condition	1BF	2BF
productivity (t m ⁻³ d ⁻¹)	2.147	2.760
blast volume (m ³)	3200	3800
top pressure (MPa)	0.2	0.28
coal injection rate (kg/t of hot metal)	151.4	183
coke injection rate (kg/t of hot metal)	361.6	335

The char samples were prepared in a bench-scale fixed furnace, which constituted a quartz tube with 1000 mm in length and 40 mm in diameter. The furnace was heated at 5 °C/min from the ambient temperature to 1500 °C in an inert atmosphere of N₂. When the stable condition was reached, a graphite sample holder containing 0.5 g of coal samples ground down 74 μm was pushed to the thermostat segment, kept for 5 min, and then cooled to room temperature. Finally, the char samples were removed to a desiccator standby. Different ratios (0, 10, 20, 30, 40, and 50%) of produced chars were mixed with drilled cokes to prepare synthetic mixtures, simulating the possible constituents of the flue dust from BF.

2.2. Sample Characterization. **2.2.1. Chemical Analyses.** Chemical and granulometric analyses of flue dusts were carried out. The dust samples were mechanically separated into seven size fractions ranging from <38 to >450 μm.¹² The separation was conducted to understand how the carbonaceous particles were distributed in the flue dust and to identify the possible sized fraction composed of char or coke or both.

2.2.2. SEM Analysis. The morphology of the dust samples was examined using SEM (Sirion 200, FEI) with the typical accelerating voltage of 20 kV.

2.2.3. Petrographical Microanalysis. The purpose of the petrographical microanalysis was to differentiate unconsumed pulverized coal and fine coke as well as other substances from the BF dust. To obtain the area ratio between the unconsumed pulverized coal and fine coke, a reflected polarized light microscope (Leica MSP-200) with the amplification of 500 was used. The “counting-points method” for the coal phase was made of use in the investigation of the percentage of areas occupied by unconsumed fine coke and pulverized coal as well as oxides in BF flue dust.^{13,14} With the statistic method, the ratio of the

unconsumed fine coke and pulverized coal as well as oxides in BF dust could be determined.²

2.2.4. Raman Spectroscopy. The Raman spectra of flue dust and chars were acquired by confocal Raman microspectroscopy (Renishaw RM-1000), using an Ar⁺ laser beam at 514.4 nm, with spectral resolution of 1 cm⁻¹. Raman spectra were measured in the range of 800–3000 cm⁻¹. Laser power at the samples of less than 0.4 MW was used as an excitation source. The parameters derived from Raman spectra, mainly I_D/I_G , I_V/I_G , and I_{2D}/I_G , were used to investigate the flue dust and its correlation to the ratio of unconsumed pulverized coal and fine coke.

2.3. Quantification Procedure. First, the flue dusts were analyzed by means of the petrographical microanalysis. The unconsumed fine coke can be divided into a block structure, hemophilic silk carbon, flowing structure, slice structure, and granule inlay structure, while the unconsumed coal was found in the form of undeformed and deformed coal.² The ratio of unconsumed coal “Γ” in dust was calculated by eqs 1–3. The correctional parameter α was defined as 0.6.¹² The synthetic mixtures were also analyzed by petrographical microanalysis to verify the accuracy of the petrographical microanalysis method.

$$\begin{aligned} \sum \text{unconsumed fine coke (\%)} \\ = \sum (\text{block structure} + \text{hemophilic silk carbon} \\ + \text{flowing structure} + \text{slice structure} \\ + \text{granule inlay structure}) (\%) \end{aligned} \quad (1)$$

$$\begin{aligned} \sum \text{unconsumed coal (\%)} \\ = \text{undeformed coal (\%)} + \alpha \sum (\text{deformed coal}) (\%) \end{aligned} \quad (2)$$

$$\begin{aligned} \Gamma = \sum \text{unconsumed coal} / (\sum \text{unconsumed fine coke} \\ + \sum \text{unconsumed coal}) \end{aligned} \quad (3)$$

The BF flue dust and synthetic mixtures were analyzed by Raman. On the basis of the evolutions of I_D/I_G , I_V/I_G , and I_{2D}/I_G obtained from Raman spectra of different synthetic mixtures, calibration curves were obtained. When I_D/I_G , I_V/I_G , and I_{2D}/I_G are compared from BF flue dust and calibration curves, the compositions of BF flue dust can be established. The compositions of BF flue dust by Raman were then compared to those by petrographical microanalysis.

3. RESULTS AND DISCUSSION

Chemical analyses of the coke, coal, and flue dust are shown in Table 2. It was noteworthy that carbon in flue dusts was high. The dust samples from 1BF and 2BF contained 39.77 and 32.11% carbon, respectively. The fuel use was only 50–70%, indicating the inferior operation condition of BF. Therefore, it was important to figure out the origin of carbonaceous materials in flue dust. (1) Unconsumed coal: within limited times and space between the exit of the injection lance and the rear wall of the raceway, combustion will invariably be incomplete, meaning that considerable amounts of char will escape the raceway region.¹⁵ (2) Unconsumed coke: coke fines were produced by

Table 2. Chemical Composition of Coal, Coke, and Dust

sample	proximate analysis (wt %)				elemental analysis (wt %)				
	M_{ad}	V_{ad}	A_{ad}	FC_{ad}	C_{ad}	H_{ad}	O_{ad}	N_{ad}	S_{ad}
1BF-PCI	1.78	17.22	10.19	70.81	80.44	2.47	3.52	1.15	0.45
1BF-MC	0.48	1.46	12.46	85.83	83.79	1.03	0.41	1.09	0.74
1BF-dust	0.70	6.79	55.36	37.15	39.77	0.99	2.39	0.46	0.33
2BF-PCI	1.30	15.46	9.79	73.45	81.30	2.33	3.56	1.28	0.44
2BF-MC	0.53	1.31	12.54	85.62	83.07	1.27	0.70	1.13	0.76
2BF-dust	0.75	6.57	64.02	28.66	32.11	1.00	1.35	0.42	0.35

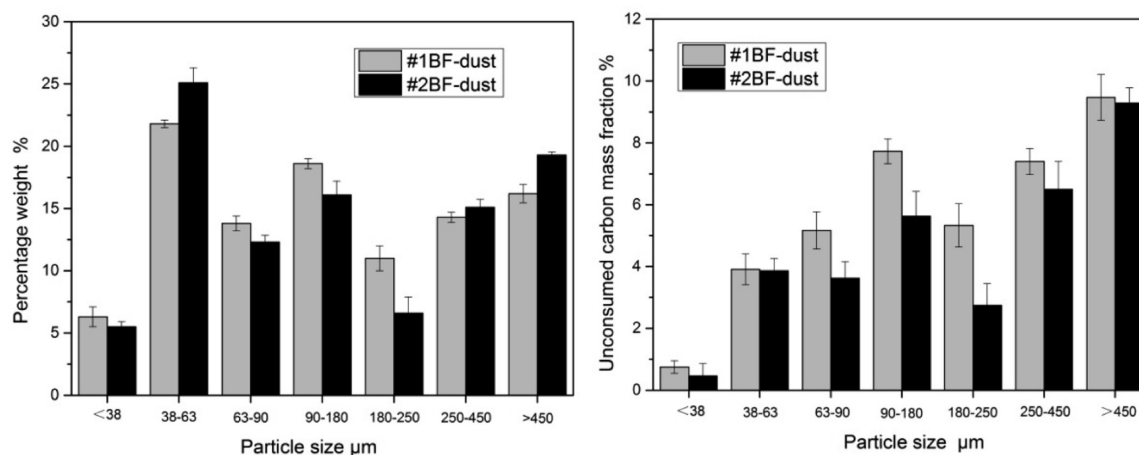


Figure 1. Particle size distribution and carbon amount of dusts from 1BF and 2BF.

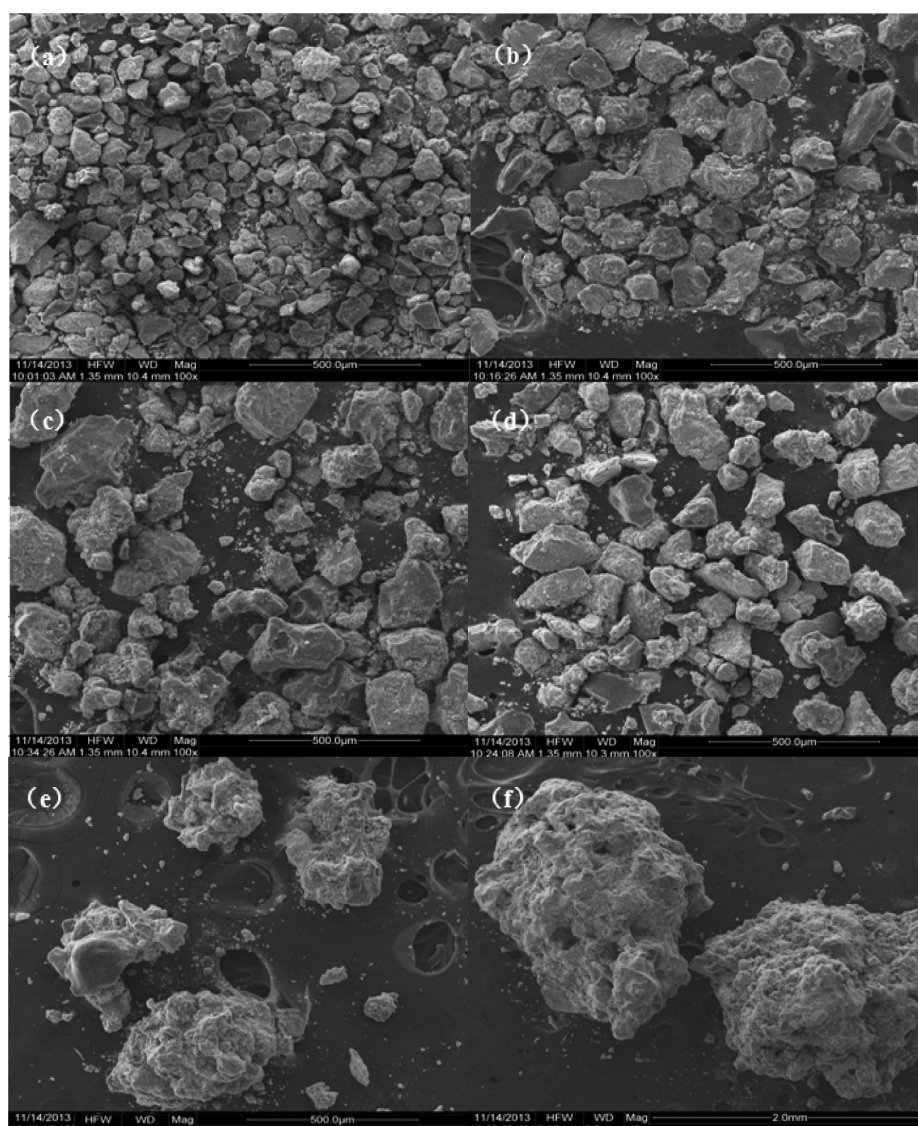


Figure 2. SEM analysis of dust from 1BF: (a) 38–63 μm , (b) 63–90 μm , (c) 90–180 μm , (d) 180–250 μm , (e) 250–450 μm , and (f) >450 μm .

mechanical impact of rotating coke, thermal stress, combustion, and solution loss reactions.^{16,17} Flue gas expansion because of rapid release and combustion of volatiles from coal may be responsible for the carryover of produced coke fines.¹⁸

Figure 1 gave the particle distribution of dust samples from 1BF and 2BF. It can be observed that the predominant fraction was in the range of 38–450 μm , accounting for 78.5 and 75.2% of all sizes for 1BF and 2BF, separately. In the BF, most fine coal

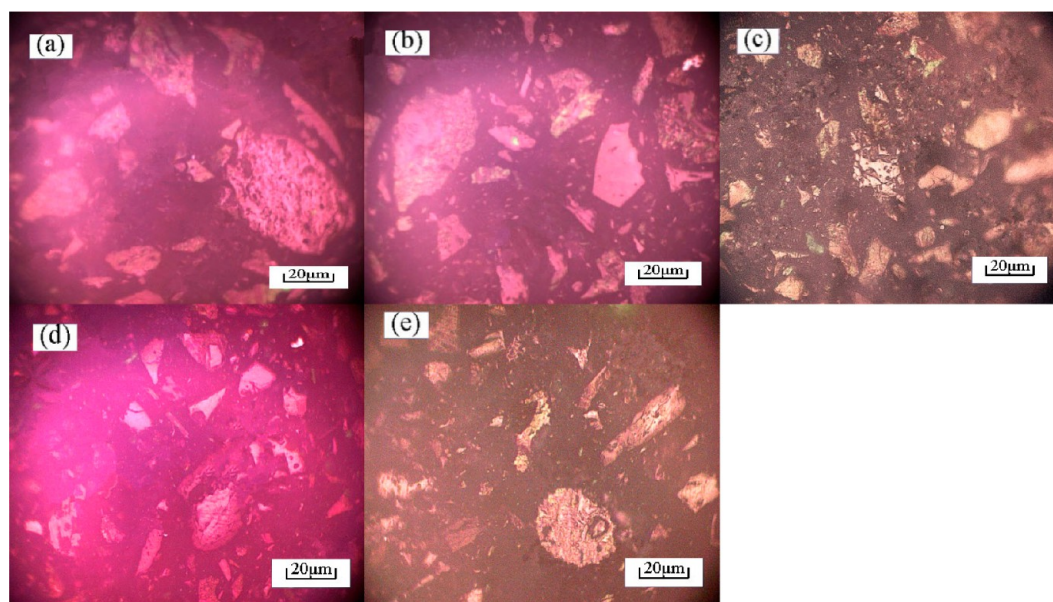


Figure 3. Microscopic observation of synthetic mixtures: (a) 10% char, (b) 20% char, (c) 30% char, (d) 40% char, and (e) 50% char.

Table 3. Percentage of Components of the Microstructure in Synthetic Mixtures (wt %)^a

sample	coke								char	
	1		2		3		4		1BF	2BF
	1BF	2BF	1BF	2BF	1BF	2BF	1BF	2BF		
10% char	11.8	8.6	60.2	73.2	2.4	1.4	15.4	8.4	10.2	8.4
20% char	10.4	6.6	53	64.6	2.4	2.8	15.8	8.8	18.4	17.2
30% char	8.6	5.2	46	54.2	1.6	2.6	11.2	7.6	32.6	30.4
40% char	8.4	4.8	36.6	48.4	1.2	1	13.2	6.4	40.6	39.4
50% char	7.2	4.4	35	42	0.6	0.2	9.2	4.6	48	48.8

^a1, block structure; 2, granule inlay structure; 3, flowing structure; 4, hemophilic silk carbon + slice structure; 5, undeformed coal; and 6, deformed coal.

particles exited from the “raceway” surface and then moved upward into the coke bed above the “raceway” rather than moving forward, because fine coal particles were easier to be affected by the flow turbulence. Then, these unconsumed coals will exist in flue dust. A high coal injection rate will boost this phenomenon. The coal used in this study was smaller than 74 μm . Therefore, the unconsumed coal mainly existed in dust particles smaller than 63 μm . Coke fines from the bosh level downward were mainly generated by sheer stress because of the increased load to the coke bed and attrition/abrasion because of upward gas flow.¹⁷ In the raceway, coke fines were produced by mechanical impact of rotating coke, thermal stress, combustion, and solution loss reactions. Some generated coke fines would be carried upward, existing in flue dust. Therefore, coke and coal fines generated in different parts of BF made the particle size of flue dust far from uniform. The carbon content in each size range of dust samples was also given in Figure 1. The amount of carbon in the dust particles less than 38 and 38–63 μm in size was insignificant and smaller than 4%. The carbon was mainly concentrated in the larger particles greater than 90 μm . According to Gupta et al.,¹⁹ the high carbon content in dust particles greater than 90 μm was associated with coke fines. The authors also assumed that the dust particles greater than 250 μm were composed exclusively of coke fines. In the present study, the particle size of coal used in two BFs was smaller than 74 μm . Therefore, considering particle size distribution and carbon in

each size range of flue dusts, it was preliminary estimated that carbonaceous materials mainly originated from coke fines.

Figure 2 provides the SEM images of the dust particles from 1BF. In Figure 2a, morphological features of dust particles appeared to be more irregular, fluffy, and sharp-edged, characteristics of typical char particles. Therefore, it was inferred that most of the carbon fines in the dust particles smaller than 63 μm were attributed to the char fines. On the other hand, dust particles larger than 250 μm indicated the clear absence of such irregular and sharp-edged char-like particles, as seen in panels e and f of Figure 2. The SEM result was consistent with chemical analysis. A similar trend of carbon fine distribution was also noted for 2BF.

To understand the characteristics of different carbonaceous materials in microscopic images and to further provide evidence for the analysis of compositions of BF flue dust, the different synthetic mixtures were analyzed by petrographical microanalysis. Moreover, the accuracy of the petrographical microanalysis method was verified by comparing the char fractions obtained through petrographical microanalysis to the actual amount in synthetic mixtures. The microscopic images of synthetic mixtures are shown in Figure 3. It can be observed that lithofacies features of synthetic mixtures containing 10 and 20% chars were characteristic of more large, regular particles and less fine, irregular particles. With the proportion of chars in synthetic mixtures increasing, the amount of larger particles gradually

decreased. Especially, the amounts of block and tiny particles were close to each other in the case of synthetic mixtures containing 50% chars. The result indicated that the coke was characteristic of block and uniform particles, while the char was marked by peaked, irregular, and tiny particles, which was consistent with the result of SEM. The results and relative error of petrographical microanalysis for synthetic mixtures are given in Tables 3 and 4.

Table 4. Components of the Synthetic Mixtures by Petrographical Microanalysis (wt %)

	sample	Γ_1	Γ_2	average value	relative error
1BF	10% char	11.2	9.2	10.2	2.0
	20% char	17.2	19.6	18.4	8.0
	30% char	34	31.2	32.6	8.7
	40% char	39.2	42	40.6	1.5
	50% char	48.4	47.6	48	4.0
2BF	10% char	8.8	9.8	8.4	7.0
	20% char	18.2	19.3	17.2	6.3
	30% char	28	30.4	29.2	2.7
	40% char	43.4	35.4	39.4	1.5
	50% char	49.8	47.8	48.8	2.4

The ratio of unconsumed coal was obtained by eqs 1–3. The relative errors for synthetic mixtures by petrographical microanalysis were all below 10%, with the minimum relative error less than 2%. The results proved that petrographical microanalysis was a reliable mean to analyze the compositions of BF flue dust.

Through petrographical microanalysis, different lithofacies features of BF flue dusts are given in Figure 4. Panels a–d of Figure 4 demonstrated anisotropy components of coke. Panels e and f of Figure 4 showed undeformed and deformed coals, and the mineral compounds in flue dust were illustrated in panels g–i of Figure 4. Table 5 gave the proportions of different components in flue dust. It can be observed that the amount of oxides showed the highest amounts being 52.83 and 56.08% for 1BF and 2BF, respectively, which were close to the results of proximate analysis of BF flue dusts, as shown in Table 2. Through petrographical microanalysis, the ratios of unconsumed coal “I” in flue dusts from 1BF and 2BF were estimated to be 9.7 and 11.6%, respectively, as shown in Table 4.

Figure 4 showed the Raman spectra of BF flue dust and synthetic mixtures after baseline corrections. It can be observed that Raman spectra of samples can be divided into first- and second-order regions. Three bands dominated the spectra and were designated as G, D, and 2D bands. Quantitative parameters from Raman spectra can be obtained from the decompositions of the spectra by fitting procedures set up following the procedures.²⁰ In the first regions, the baseline-corrected spectrum was deconvoluted into two bands centered at 1595 and 1355 cm^{-1} , where the G and D bands lied, respectively. The G band rose from the E_{2g} vibrational modes, which were ascribed to the sp^2 -bonded carbon in the hexagonal graphitic planes and assigned to the normal graphite structure.²⁰ Therefore, the G band was regarded as the Raman scattering from the inner graphitic plane.

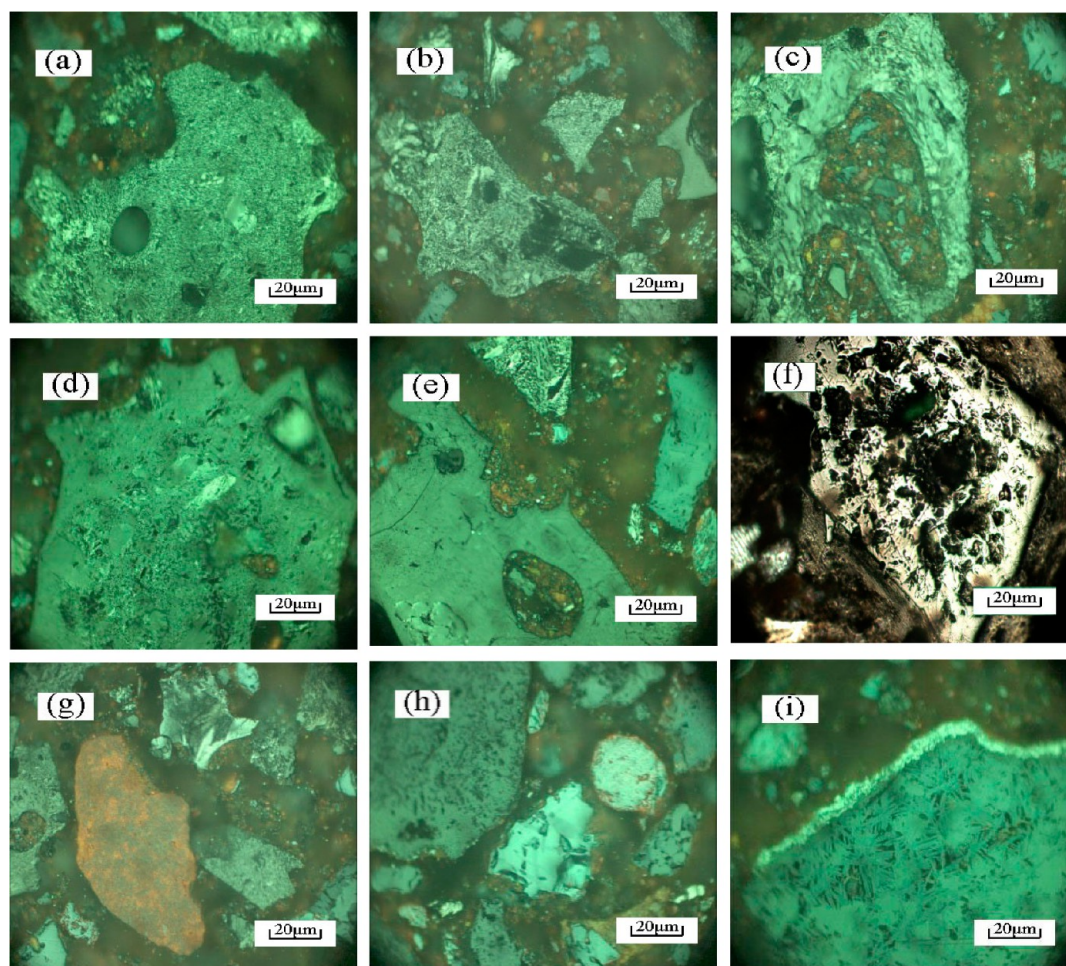


Figure 4. Microscopic observation of the 1BF dust.

Table 5. Percentage of Components of the Microstructure in BF Dust (wt %)^a

sample	coke				Σ_{coke}	unconsumed coal		$\Sigma_{\text{unconsumed coal}}$	oxides	Γ
	1	2	3	4		5	6			
1BF	6.10	20.68	1.92	14.11	42.81	4.02	0.57	4.36	52.83	9.7
2BF	7.24	18.3	2.18	11.7	39.42	3.51	1.64	4.50	56.08	11.6

^a1, block structure; 2, granule inlay structure; 3, flowing structure; 4, hemophilic silk carbon + slice structure; 5, undeformed coal; and 6, deformed coal.

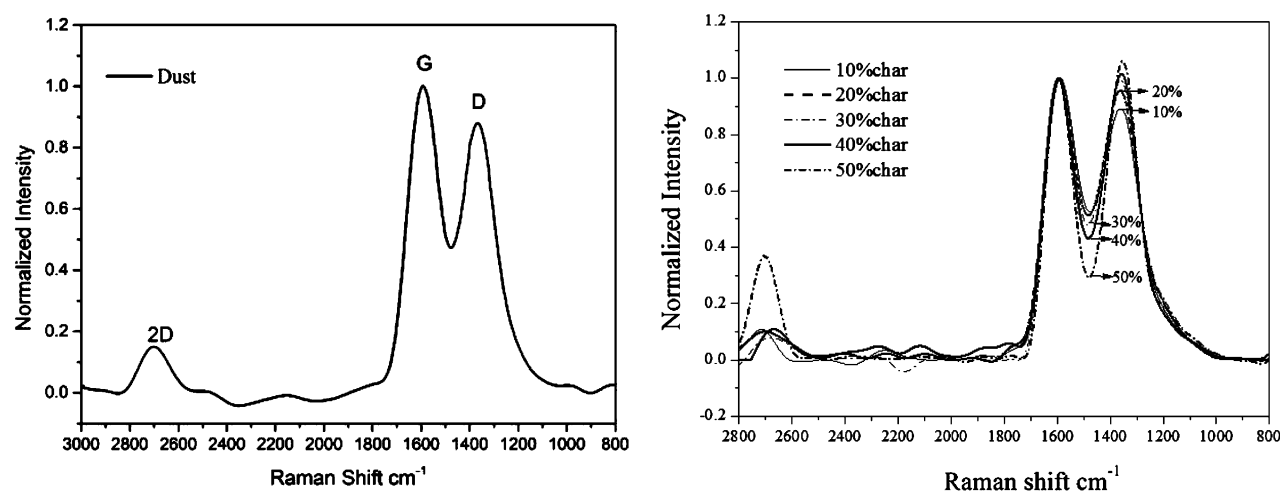


Figure 5. Normalized Raman spectra of dust and synthetic mixtures for 1BF.

The D band was associated with the disordered and strongly distorted structure of turbostratic carbon, the graphitic defect fractions of the samples.²¹ The D band intensity depended upon breaking of crystalline symmetry²² and grew in intensity relative to the G band with an increasing degree of disorder in the graphitic structure.²³ Two other bands at ~ 1500 and ~ 1200 cm^{-1} (designated as V and D1) were needed to reproduce the original measured spectra. The V band generally appeared as a very broad band around 1500 – 1550 cm^{-1} , which was suggested to originate from the amorphous sp^2 -bonded forms of carbon, such as organic molecules, fragments, or functional groups, in poorly organized materials.⁹ The D1 band appeared only in poorly organized materials, such as soot and coal chars,²³ which was attributed to sp^3 – sp^2 mixed sites at the periphery of crystallites or C–C and C=C stretching vibrations of polyene-like structures. In this way, the original spectrum was represented by a combination of G, D, V, and D1 bands. A second-order Raman spectrum 2D can also be used to characterize disorder in carbon materials. The 2D band has been attributed to the overtone of the D band and was strongest for the most ordered graphitic structure.¹¹ The main features in the spectrum were at 2700 cm^{-1} . It was important to emphasize that the second-order Raman spectra were in part due to structural disorder and were expected to be more sensitive to disorder changes.²² It was found that the 2D band was inclined to broaden and shift to lower wavenumbers or even disappear when the carbon structure became less ordered.²⁴

On the basis of the above interpretation of the nature of the bands, three spectral parameters ($I_{\text{D}}/I_{\text{G}}$, $I_{\text{V}}/I_{\text{G}}$, and $I_{2\text{D}}/I_{\text{G}}$) can be defined. It was believed that $I_{\text{D}}/I_{\text{G}}$ was related to the crystallite size. An increase in carbon crystallinity can be expressed by a decrease in the d spacing (d_{002}) and an increase in crystallite height (L_{c}) and width (L_{a}). It was reported that $I_{\text{D}}/I_{\text{G}}$ was proportional to the crystal planar domain size ($I_{\text{D}}/I_{\text{G}} \propto L_{\text{a}}$)⁸ for crystallite sizes L_{a} lower than 2 nm and increased for increasing crystallinity. The $I_{2\text{D}}/I_{\text{G}}$ can be also used as an alternative

technique to clearly quantify the difference in crystallinity. It was noteworthy that the intensity ratio of bands estimated different fractions by volume in flue dust and mixtures. The density of individual carbonaceous substances in studied samples showed little difference. Under the above assumption, the volume ratio equaled the mass fractions approximately.

Normalized Raman spectra of synthetic mixtures for 1BF are shown in Figure 5. Clear differences can be observed in both the first- and second-order regions. On the basis of the discussion above, the intensity ratios of the 2D to G band, the D to G band, and the valley between G and D bands to G band can be used to estimate the compositions of the synthetic mixtures. The G and D bands were found to become sharper as the char amount in synthetic mixtures increased. $I_{\text{D}}/I_{\text{G}}$ and $I_{2\text{D}}/I_{\text{G}}$ were observed to increase when the amount of chars in synthetic mixtures increased, which indicated a more ordered synthetic mixture with the amount of chars increased. Dong et al.¹¹ pointed out that the Raman intensity was proportional to the percentage of the “boundaries” in the samples and the increase in edge density because an increase in the average number of graphitic planes in the stacking crystallite gave a higher intensity of the D band. The ordering of samples was also reflected by the decrease in intensity of $I_{\text{V}}/I_{\text{G}}$. The above tendency was accompanied by the width narrowing of the G, D, and 2D bands when the mass ratio of chars in synthetic mixtures increased. The observed width narrowing of D and G bands suggested a more uniformed and homogenized carbon structure, resulting from a decrease in both the concentrations and distribution of amorphous carbon structures.

Figures 6 and 7 estimated the compositions of BF flue dusts from 1BF and 2BF by means of $I_{\text{D}}/I_{\text{G}}$, $I_{\text{V}}/I_{\text{G}}$, and $I_{2\text{D}}/I_{\text{G}}$. Through this method, the mass ratio of chars to carbonaceous matter in flue dusts from 1BF and 2BF were estimated to be in the ranges of 8 – 10 and 10.5 – 12% , respectively, which were consistent with results of petrographical microanalysis, being 9.7 and 11.6% for

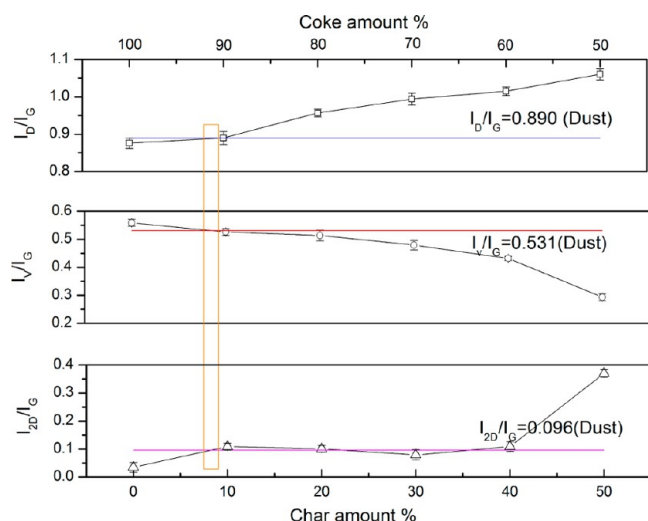


Figure 6. I_D/I_G , I_V/I_G , and I_{2D}/I_G of different synthetic mixtures and dust from 1BF.

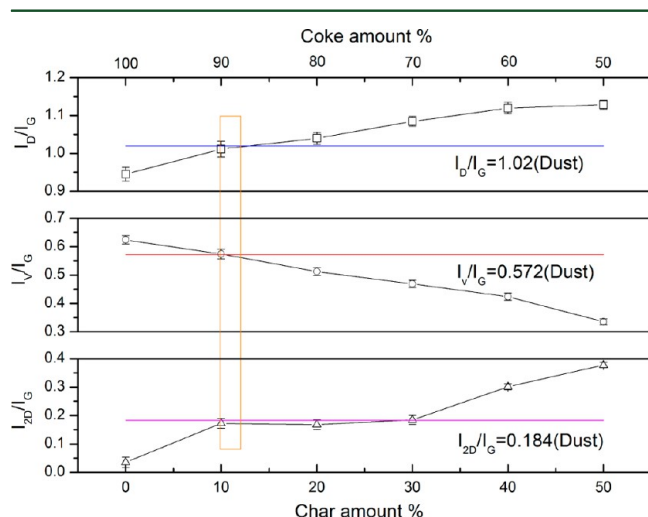


Figure 7. I_D/I_G , I_V/I_G , and I_{2D}/I_G of different synthetic mixtures and dust from 2BF.

1BF and 2BF, respectively. Accordingly, the mass ratios of coke to carbonaceous matter in flue dusts were in the ranges of 90–92 and 88–89.5% for 1BF and 2BF, respectively. Further, the char and coke ratios in flue dust can be established by the above results and the proximate analyses of flue dust shown in Table 2. Through the analysis, quantitative analyses of two sets of synthetic mixtures have demonstrated the promising possibility that Raman spectroscopy may be developed into a relatively rapid monitoring technique for the purpose of differentiation between coke and chars. Such knowledge was useful in determining the extent to which injectant coal was effectively converted within the BF. The potential for regular monitoring of the carbon content of flue dust offered a significant improvement on the current laborious point-counting method.

4. CONCLUSION

This paper investigated the percentage of unconsumed pulverized coal and coke in flue dust by means of chemical and petrographical microanalyses and Raman spectra. The following conclusions were drawn: (1) The predominant fraction of flue dusts was in the range of 38–450 μm size fractions, accounting

for 78.5 and 75.2% of all sizes for 1BF and 2BF, separately. With the integration of particle size distribution and carbon in each size range of flue dusts, carbonaceous material was preliminarily estimated to originate from coke fines. (2) The unconsumed coke was divided into a bloke structure, hemophilic silk carbon, flowing structure, slice structure, and granule inlay structure. While unconsumed coal was divided into undeformed and deformed coals. Through petrographical microanalysis, the ratios of unconsumed coal “T” in flue dusts from 1BF and 2BF were estimated to be 9.7 and 11.6%, respectively. (3) The parameters obtained from Raman spectra, I_D/I_G and I_{2D}/I_G , were observed to increase when the amount of chars in synthetic mixtures increased, while I_V/I_G showed an opposite trend. In comparison of the ratios of the band intensity of synthetic mixtures and flue dusts, the mass ratios of chars in flue dusts from 1BF and 2BF were estimated to be in the ranges of 8–10 and 10.5–12%, respectively, which were consistent with the results of petrographical microanalysis.

It was concluded that Raman spectroscopy may be developed into a relatively rapid, efficient, and accurate monitoring technique for the purpose of differentiation between coke and chars, with decreasing manpower cost compared to petrographical microanalysis.

AUTHOR INFORMATION

Corresponding Author

*Telephone: +86-27-87542417-8207. Fax: +86-27-87545526. E-mail: sunlushi@hust.edu.cn.

Notes

The authors declare no competing financial interest.

ACKNOWLEDGMENTS

This work was supported by the Natural Science Foundation of China (51376073). The authors thank the Analytical and Testing Center of Huazhong University of Science and Technology for assisting with the analysis work.

REFERENCES

- (1) Babich, A.; Senk, D.; Gudenau, H. W.; Mavrommatis, K. *Ironmaking*; Mainz GmbH: Aachen, Germany, 2008; pp 402.
- (2) Wu, K.; Ding, R.; Han, Q.; Yang, S.; Wei, S.; Ni, B. Research on unconsumed fine coke and pulverized coal of BF dust under different PCI rates in BF at Capital Steel Co. *ISIJ Int.* **2010**, *50*, 390–395.
- (3) Akiyama, T.; Kajiura, Y. *Advanced Pulverized Coal Injection Technology and Blast Furnace Operation*; Elsevier Science, Ltd.: Amsterdam, Netherlands, 2000; pp 169–215.
- (4) Gupta, S.; Sahajwalla, V.; Chaubal, P.; Youmans, T. Carbon structure of coke at high temperatures and its influence on coke fines in blast furnace dust. *Metall. Mater. Trans. B* **2005**, *36*, 385–394.
- (5) Ueno, H.; Yamaguchi, K.; Tamura, K. Coal combustion in the raceway and tuyere of a blast furnace. *ISIJ Int.* **1993**, *33*, 640–645.
- (6) Yamaguchi, K.; Ueno, H.; Tamura, K. Maximum injection rate of pulverized coal into blast furnace through tuyeres with consideration of unburnt char. *ISIJ Int.* **1992**, *32*, 716–724.
- (7) Machado, A. d. S.; Mexias, A. S.; Vilela, A. C. F.; Osorio, E. Study of coal, char and coke fines structures and their proportions in the off-gas blast furnace samples by X-ray diffraction. *Fuel* **2013**, *114*, 224–228.
- (8) Zickler, G. A.; Smarsly, B.; Gierlinger, N.; Peterlik, H.; Paris, O. A reconsideration of the relationship between the crystallite size L_a of carbons determined by X-ray diffraction and Raman spectroscopy. *Carbon* **2006**, *44*, 3239–3246.
- (9) Sheng, C. Char structure characterised by Raman spectroscopy and its correlations with combustion reactivity. *Fuel* **2007**, *86*, 2316–2324.
- (10) Wang, M.; Roberts, D. G.; Kochanek, M. A.; Harris, D. J.; Chang, L.; Li, C.-Z. Raman spectroscopic investigations into links between

intrinsic reactivity and char chemical structure. *Energy Fuels* **2013**, *28*, 285–290.

(11) Dong, S.; Paterson, N.; Kazarian, S. G.; Dugwell, D. R.; Kandiyoti, R. Characterization of tuyere-level core-drill coke samples from blast furnace operation. *Energy Fuels* **2007**, *21*, 3446–3454.

(12) Sahajwalla, V.; Gupta, S. *PCI Coal Combustion Behavior and Residual Coal Char Carryover in the Blast Furnace of 3 American Steel Companies during Pulverized Coal Injection (PCI) at High Rates*; American Iron and Steel Institute: Washington, D.C., 2005.

(13) Ministry of Metallurgical Industry of China. YB/T 077-1995. *Method of Determining Optical Texture of Coke*; Ministry of Metallurgical Industry of China: Beijing, China, 1996.

(14) Ministry of Metallurgical Industry of China. GB/T 8899-1998. *Determination of Maceral Group Composition and Minerals in Coal*; Ministry of Metallurgical Industry of China: Beijing, China, 1998.

(15) Mathieson, J. G.; Truelove, J. S.; Rogers, H. Toward an understanding of coal combustion in blast furnace tuyere injection. *Fuel* **2005**, *84*, 1229–1237.

(16) Shen, Y.; Shiozawa, T.; Austin, P.; Yu, A. Model study of the effect of bird's nest on transport phenomena in the raceway of an ironmaking blast furnace. *Miner. Eng.* **2014**, *63*, 91–99.

(17) Leimalm, U.; Lundgren, M.; Ouml; Kvist, L. S.; Bj; Rkman, B. Off-gas dust in an experimental blast furnace, Part 1: Characterization of flue dust, sludge and shaft fines. *ISIJ Int.* **2010**, *50*, 1560–1569.

(18) Zou, C.; Wen, L.; Zhang, S.; Bai, C.; Yin, G. Evaluation of catalytic combustion of pulverized coal for use in pulverized coal injection (PCI) and its influence on properties of unburnt chars. *Fuel Process. Technol.* **2014**, *119*, 136–145.

(19) Gupta, S.; Sahajwalla, V.; Al-Omari, Y.; Saha-Chaudhury, N.; Rorick, F.; Hegedus, G.; Chaubala, P.; Burgo, J.; Best, M.; Hyle, F. Atomic structure of coke fines in blast-furnace dust and their origin in operating blast furnaces. *Proceedings of the 62nd Ironmaking Conference*; Indianapolis, IN, April 27–30, 2003.

(20) Kawakami, M.; Karato, T.; Takenaka, T.; Yokoyama, S. Structure analysis of coke, wood charcoal and bamboo charcoal by Raman spectroscopy and their reaction rate with CO₂. *ISIJ Int.* **2005**, *45*, 1027–1034.

(21) Paris, O.; Zollfrank, C.; Zickler, G. A. Decomposition and carbonisation of wood biopolymers—A microstructural study of softwood pyrolysis. *Carbon* **2005**, *43*, 53–66.

(22) Zaida, A.; Bar-Ziv, E.; Radovic, L. R.; Lee, Y.-J. Further development of Raman microprobe spectroscopy for characterization of char reactivity. *Proc. Combust. Inst.* **2007**, *31*, 1881–1887.

(23) Sadezky, A.; Muckenhuber, H.; Grothe, H.; Niessner, R.; Pöschl, U. Raman microspectroscopy of soot and related carbonaceous materials: Spectral analysis and structural information. *Carbon* **2005**, *43*, 1731–1742.

(24) Mennella, V.; Monaco, G.; Colangeli, L.; Bussoletti, E. Raman spectra of carbon-based materials excited at 1064 nm. *Carbon* **1995**, *33*, 115–121.